Investigations on the solid state interaction between LiAlH$_4$ and NaNH$_2$

Yong Shen Chua [b], Guotao Wu [a], Zhitao Xiong [a,*], Ping Chen [a,b]

[a] Dalian Institute of Chemical Physics, Dalian 116023, China
[b] Department of Chemistry, National University of Singapore, Singapore 117542, Singapore

ARTICLE INFO

ABSTRACT

In this paper, two LiAlH$_4$–NaNH$_2$ samples with LiAlH$_4$ to NaNH$_2$ molar ratio of 1/2 and 2/1 were investigated, respectively. It was observed that both samples evolved 2 equiv H$_2$ in the ball milling process, however, the reaction pathways were different. For the LiAlH$_4$–NaNH$_2$ (1/2) sample, Li$_3$Na(NH$_2$)$_4$ and NaAlH$_4$ were formed through cation exchange between reactants. The NaAlH$_4$ formed further reacts with Li$_3$Na(NH$_2$)$_4$ and NaNH$_2$ to give H$_2$, NaH and LiAlN$_2$H$_2$. For the LiAlH$_4$–NaNH$_2$ (2/1) sample, Li$_3$Na(NH$_2$)$_4$, LiNH$_2$ and NaAlH$_4$ were formed firstly through the same cation exchange process. The resulting LiNH$_2$ reacts with the remaining LiAlH$_4$ and produces H$_2$ and Li$_2$AlNH$_2$.

1. Introduction

The depletion of fossil fuel has aroused tremendous efforts in building a new energy system. Because of its abundance, high energy output and zero emission hydrogen is recognized as the most prospective energy carrier in the future energy system. A typical hydrogen cycle is composed of hydrogen production, hydrogen delivery and the conversion of hydrogen to electricity or thermal energy. Pipeline can be used to supply hydrogen to stationary users, while for mobile application, hydrogen has to be stored on-board. Hydrogen storage is one of the key technological challenges in building an efficient, hydrogen-powered fuel cell vehicle. Several potential storage systems such as complex hydrides [1,2], metal organics frameworks (MOFs) [3,4], ammonia borane [5,6] and so forth, have been developed recently to meet the gravimetric and volumetric density requirements. One of the prospective solid storage systems is the amide–hydride combination which was brought out based on the discovery of hydrogenation of Li$_3$N [7]. Various combinations of amides and hydrides were found capable of evolving hydrogen at temperatures lower than those for the thermal decomposition of amide and hydride individuals [8–11]. Driving force for the solid state amide–hydride interaction was mainly attributed to high potential for the combination of H$^{\delta+}$ in amide and H$^{\delta-}$ in hydride [12]. In addition, the attraction between N in amide and cation in hydride was also considered responsible for the occurrence of interaction [12]. Very recently, complex hydrides e.g. LiAlH$_4$ were brought into amide–hydride system. Owing to its

electron-rich hydrogen atoms, [AlH$_4$]$^-$ anion in LiAlH$_4$ will act as hydride source. Several authors recently focused on interactions between Li(Na)NH$_2$ and Li(Na)AlH$_4$ at varied molar ratios, with the hope to obtain a reversible system. Xiong et al. investigated LiNH$_2$–LiAlH$_4$ (1/1) [13] and (2/1) [14] system and reported that the formal system is able to detach 8 wt% of H$_2$, but none of those H$_2$ can be recharged under 80 bars of H$_2$ pressure. LiNH$_2$–LiAlH$_4$ (2/1) system on the other hand is able to detach 2 equiv H$_2$ after 12 hours of ball milling to form a Li–Al–N–H complex which can reversibly store 5.17 wt% of H$_2$. Relevant work was done by Nakamori et al. [15] in the LiNH$_2$–LiAlH$_4$ (2/1) system. In the study of LiNH$_2$–LiAlH$_4$ (1/2) system Jun and Fang [16] reported that LiNH$_2$ functions as a destablizer, like other catalysts i.e. TiCl$_3$–1/3AlCl$_3$ which effectively promotes the decomposition of LiAlH$_4$. Other combination of amides-complex hydrides, i.e., LiNH$_2$–LiAlH$_4$, LiNH$_2$–NaAlH$_4$, NaNH$_2$–LiAlH$_4$ and NaNH$_2$–NaAlH$_4$, were also studied by Dolotko et al. [17].

Among a wide range of amides–complex hydrides combinations, interaction between NaNH$_2$ and LiAlH$_4$ is of particular interest. Our previous investigations on LiAlH$_4$–NaNH$_2$ system (LiAlH$_4$–NaNH$_2$ molar ratio 1/1) revealed that 2 equiv H$_2$ or 5.2 wt% hydrogen can be evolved upon mechanical milling or heating these two chemicals at ca. 120 °C [9]. The evolution was a strong exothermic reaction and as a result, reversibly storing hydrogen on this system was not thermodynamically favored. However, the rate of hydrogen release is remarkably faster than most of the complex and chemical hydrides. In this study, we varied the molar ratio of LiAlH$_4$/NaNH$_2$ to 1/2 and 2/1 in hope that compositional change in the starting mixture will lead to a different reaction pathway and thus alter the thermodynamics and kinetics of hydrogen evolution. Our experimental results showed that a total of 2 equiv H$_2$ can be

* Corresponding author. Fax: +86 84685940.
E-mail address: xzt@dicp.ac.cn (Z. Xiong).

released from the two LiAlH$_4$/NaNH$_2$ mixtures in the process of ball milling. The reaction pathways were uncovered as a result of detailed XRD, FTIR and NMR characterizations on those species formed in the milling process. It was observed that LiAlH$_4$ and NaNH$_2$ firstly underwent cation exchange to form intermediates prior to dehydrogenation. At the end of dehydrogenation (upon releasing 2 equiv H$_2$) two complexes, i.e., LiAlN$_2$H$_2$ (1/2 ratio) and Li$_2$AlNH$_2$ (2/1 ratio), were formed.

2. Experimental methods

2.1. Sample preparations

LiAlH$_4$ and NaNH$_2$ were Fluka products with claimed purities of 97% and 95%, respectively, and were used as received. LiAlH$_4$–NaNH$_2$ mixtures with LiAlH$_4$/NaNH$_2$ molar ratio 1/2 and 2/1 (denoted as S-I and S-II) were mechanically milled on a Retsch PM 400 mill at 200 rpm. The ball to sample ratio was about 30:1. At the milling interval, the milling vessel was connected to a pressure gauge to measure the gas pressure inside. Gaseous product was also conducted to a mass spectrometer (MS) for analysis and in all case only hydrogen was detectable. For comparison, LiAlH$_4$ was milled alone at same conditions for up to 50 hours and negligible amount of hydrogen was evolved, in consistent with the literature reports [18,19]. NaNH$_2$ is stable too against ball milling. All the sample handlings were carried out within a MBRAUN glove-box which was filled with purified argon to prevent air and moisture contaminations.

2.2. Sample characterizations

To understand the mechanism for hydrogen evolution from the LiAlH$_4$–NaNH$_2$ system, samples collected at different ball milling intervals were characterized by Fourier transform infrared (FTIR), X-ray diffraction (XRD) and solid state nuclear magnetic resonance (NMR). FTIR spectra were recorded by a Perkin-Elmer 3000 FTIR spectrometer at room temperature. Diffuse reflectance IR Fourier transform (DRIFT) mode was applied. Structural identifications were performed by using a Bruker D8 advanced diffractometer equipped with an in situ cell. XRD data were collected from 10° to 60° with a scan-step width of 0.01° using CuKα radiation. Sample in pellet was placed on platinum holder and occasionally diffraction peaks of platinum were observed. Chemical shifts for ^{27}Al, ^{23}Na and ^{7}Li nuclei were recorded on a DRX400 Bruker spectrometer by referring to 1.0 M of aluminum nitrate Al(NO$_3$)$_3$, sodium chloride (NaCl) and lithium chloride (LiCl) aqueous solutions. Samples were packed in 4 mm magic-angle spinning (MAS) zirconia rotors with a Kel-F cap inside the glovebox. NMR spectra were acquired in a cross-polarization (CP)/MAS probe using single-pulse excitation and a rotor-spinning rate of 10 kHz. The post-milled samples were subject to temperature programmed desorption (TPD) and differential scanning calorimeter (DSC) measurements. Briefly, samples of ca. 50 mg was loaded onto the homemade TPD system and heated at a ramping rate 2 °C/min. Purified argon was used as carrier gas to bring the gaseous products to a MS where mass channels of H$_2$, NH$_3$, N$_2$ and water were monitored. ca. 10 mg samples were tested in a Netzsch DSC 204 HP unit. Sample was heated at 2 °C/min in argon flow.

3. Results and discussion

The time dependence of pressure risings inside the milling vessel were monitored for the S-I and S-II samples. As shown in Fig. 1 gas was evolved gradually with the progress of solid-state
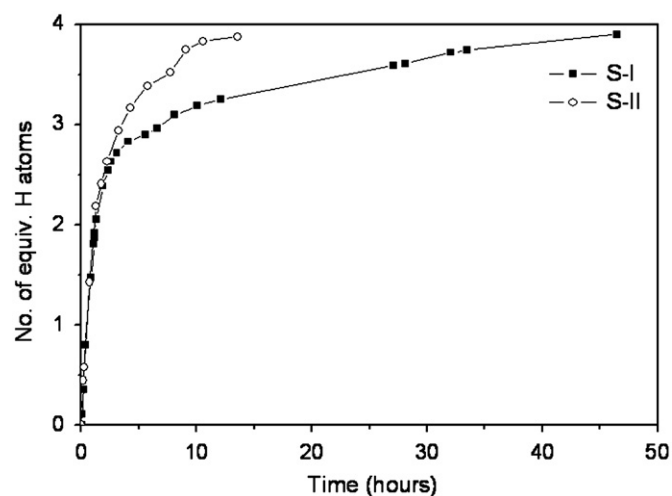

Fig. 1. Time dependences of hydrogen evolution from S-I and S-II sample in the ball milling process.

reaction between LiAlH$_4$ and NaNH$_2$. MS analysis revealed that hydrogen was the only detectable gaseous product. Therefore, by applying the ideal gas equation the amount of hydrogen evolved can be measured quantitatively. Ball milling the S-I sample for 46 hours resulted in the evolution of ca. 3.9 equiv H atoms, while S-II sample released the same amount of H$_2$ in just 14 hours of ball milling. Such difference in the reaction rate hints that changing the LiAlH$_4$/NaNH$_2$ molar ratio in the starting mixture should induce different reaction pathway. By taking into account of the purities of starting chemicals, 2 equiv H$_2$ were evolved from the above two samples, identical to that evolved from the LiAlH$_4$/NaNH$_2$ (1/1) sample. It is important to note that LiAlH$_4$ alone cannot decompose to give off H$_2$ under the identical ball milling conditions, therefore, an interaction between NaNH$_2$ and LiAlH$_4$ should take place leading to the evolution of hydrogen.

To obtain more details on the mechanism of hydrogen evolution from the S-I and S-II samples the milling process was intentionally terminated at several milling intervals, i.e., stages 1, 2, 3 and 4 correspond to the milling intervals where ca. 1, 2, 3 and 4 equiv H atoms were evolved, respectively. The milling intermediates were then collected and subjected to FTIR, XRD and solid NMR characterizations. LiAlH$_4$ and NaNH$_2$ were also mixed simply by mortar and pestle and the resulting mixture was investigated for comparison. As shown in Fig. 2 S-I sample at stage 1 displayed characteristic N–H stretches of NaNH$_2$ and two other absorbances at 3294 and 3240 cm^{-1} which were assigned to the N–H stretches of ternary amide, Li$_3$Na(NH$_2$)$_4$ [20]. In the case of S-II sample, Li$_3$Na(NH$_2$)$_4$ was also observed at initial milling stage but it were consumed rapidly. NaNH$_2$ in S-II was totally disappeared at the stage 1 while N–H stretches of LiNH$_2$ emerged. XRD characterizations (Figs. 3 and 4) at the stage 1 revealed the appearance of NaAlH$_4$ in both samples. Summarizing FTIR and XRD results a stoichiometric ionic exchange would therefore appear as Eq. (1)

$$LiAlH_4 + NaNH_2 \rightarrow LiNH_2 + NaAlH_4 \qquad (1)$$
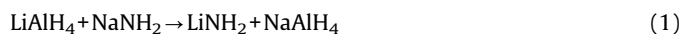
With standard enthalpy of formation of each reactant the enthalpy change of reaction (1) was calculated to be −54.9 kJ/mol, an exothermic reaction that is thermodynamically allowed at ambient milling condition. The formation of Li$_3$Na(NH$_2$)$_4$ should be the result of further reaction of LiNH$_2$ with NaNH$_2$, as shown in Eq. (2)
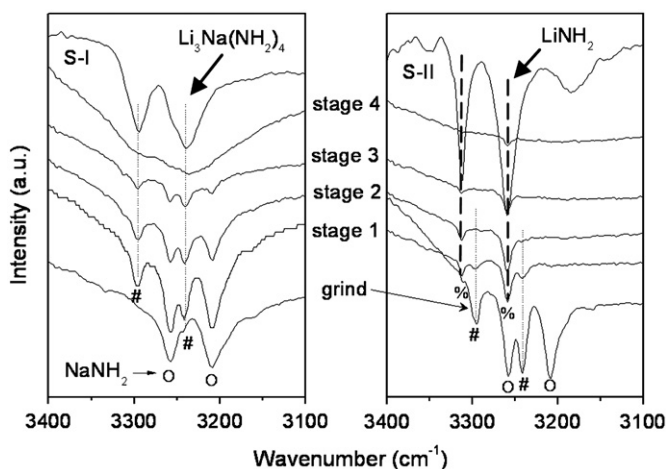
$$NaNH_2 + 3LiNH_2 \rightarrow Li_3Na(NH_2)_4 \qquad (2)$$

Fig. 2. FTIR spectra of S-I and S-II samples collected at different milling stages. # represents the N–H absorbances in $Li_3Na(NH_2)_4$, % $LiNH_2$, o $NaNH_2$.

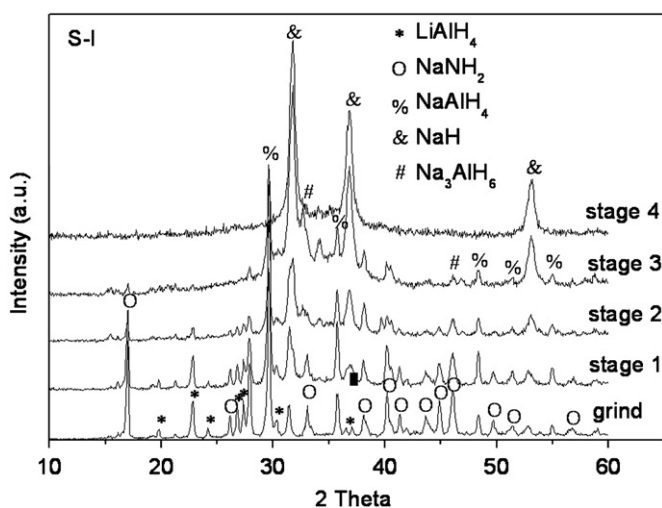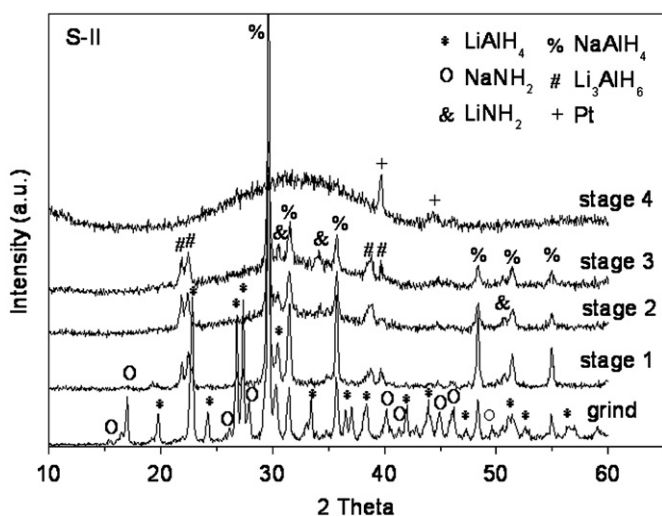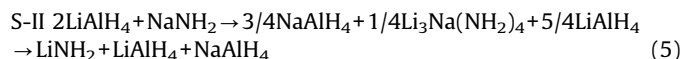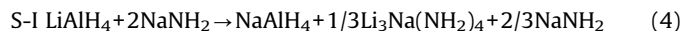**Fig. 3.** XRD patterns of S-I sample collected at different milling stages.

Fig. 4. XRD patterns of S-II sample collected at different milling stages. Platinum sample holder was observed occasionally.

To verify this, a $LiNH_2 - NaNH_2$ mixture of $LiNH_2/NaNH_2$ molar ratio of 3/1 was ball milled under the same conditions and it was found that following the vanishment of N–H stretches of $NaNH_2$ and $LiNH_2$ those absorbances at 3294 and 3240 cm^{-1} appeared, evidencing the formation of $Li_3Na(NH_2)_4$. Although the thermodynamic parameter of $Li_3Na(NH_2)_4$ is unknown, the overall Gibbs free energy change for the reaction (2) should be negative. However, XRD characterization could not present distinct pattern of this ternary amide indicating that this material can be easily deformed upon mechanical ball milling. Eq. (3) was obtained after combining Eqs. (1) and (2)

$$3LiAlH_4 + 4NaNH_2 \rightarrow 3NaAlH_4 + Li_3Na(NH_2)_4 \qquad (3)$$

Therefore, with the understanding that N–H stretches of $NaNH_2$ and $Li_3Na(NH_2)_4$ are detected in S-I sample where $NaNH_2$ is excessive, while in the S-II N–H stretches of $LiNH_2$, instead of $NaNH_2$, is observed the reaction processes at the early stage of ball milling S-I and S-II samples can be expressed by Eqs. (4) and (5), respectively.

$$\text{S-I} \quad LiAlH_4 + 2NaNH_2 \rightarrow NaAlH_4 + 1/3Li_3Na(NH_2)_4 + 2/3NaNH_2 \qquad (4)$$

$$\begin{aligned} \text{S-II} \quad & 2LiAlH_4 + NaNH_2 \rightarrow 3/4NaAlH_4 + 1/4Li_3Na(NH_2)_4 + 5/4LiAlH_4 \\ & \rightarrow LiNH_2 + LiAlH_4 + NaAlH_4 \end{aligned} \qquad (5)$$

With the progress of ball milling more hydrogen was evolved, the IR bands of $Li_3Na(NH_2)_4$ and $NaNH_2$ were getting weakened and eventually disappeared in both S-I and S-II systems. $LiNH_2$ emerged in the S-II and then disappeared too. A broad band in the range 3200–3350 cm^{-1} was developed in the post-milled S-I sample, indicating the formation of an imide-like compound [11,21]. From the XRD characterizations it is interesting to see that along with the progress of hydrogen evolution $NaAlH_4$ in the S-I sample and $LiAlH_4$ in the S-II sample were gradually consumed. Their degradation products, Na_3AlH_6 and Li_3AlH_6, were observed obviously in the mid of dehydrogenation process. At the final stage no more hydrogen was evolved in the milling process NaH was the only detectable phase in the S-I sample; while no distinct phase can be identified in the S-II sample. A broadband is presented in the range 20–50°, indicating the existence of amorphous structures (see Figs. 3 and 4) in the sample.

Solid state magic angle spinning NMR (MAS NMR) was then employed to detect the changes in chemical environment of ^{23}Al, ^{23}Na and ^{7}Li nuclei in the milling process. Shown in Fig. 5 is the ^{27}Al NMR spectrum. It can be seen that at the stage 2 both S-I and S-II samples displayed a peak at around −43.6 ppm and a broad resonance in the region of 80–120 ppm. The former resonance was assigned to Al in $[AlH_6]$ [3,22] evidencing the formation of Na_3AlH_6 (in S-I system) and Li_3AlH_6 (in S-II system) which are in good agreement with the XRD observations. Through curve fitting the broad resonance in the region of 80–120 ppm is composed of two overlapping sites centralizing at ca. 95 and 108 ppm, respectively. The resonance at ca. 95 ppm was assigned to the Al in $[AlH_4]^-$ (can be $LiAlH_4$ [22] or $NaAlH_4$ [23]). The resonance at 108 ppm is at a position between the chemical shift of Al in AlN_4 (112 ppm) [14,24] and Al in $[AlH_4]^-$, suggesting that Al may exist in a coordinated environment of $[AlH_{4-x}N_x]$. Similar assignment was given in previous investigations on the $LiAlH_4 - LiNH_2$ system [14]. The appearance of $[AlH_{4-x}N_x]$ site announces the formation of chemical bonding between Al and N. As prolonging the ball milling $[AlH_6]^{3-}$ resonance was gradually disappeared. The majority of Al species at the end of ball milling was $[AlH_{4-x}N_x]$ for the S-I sample and a mixture of $[AlH_4]^-$ and $[AlH_{4-x}N_x]$ for the S-II sample. ^{23}Na NMR spectra showed that the

Fig. 5. Solid ^{27}Al, ^{23}Na and ^{7}Li NMR spectra of S-I and S-II samples collected at milling stage 2 and 4.

Na species in S-I sample were NaH and NaAlH$_4$ at the stage 2 and NaH at the stage 4, respectively. For the S-II sample, only Na in NaAlH$_4$ was detectable in both 2 and 4 stages. The disappearance of NaAlH$_4$ from the XRD characterization (at the stage 4) is probably due to the energetic ball milling which destruct the crystal into an amorphous state. In this context, [AlH$_{4-x}$N$_x$] anion should bond with Li in both S-I and S-II samples. Accordingly, the chemical shift for ^{7}Li in the stage 4 was found around 2.21 ppm in S-I sample and 0.57 ppm in the S-II, which are different from each other and from that of LiNH$_2$ (2.38 ppm).

On the basis of FTIR, XRD and solid state NMR characterization results, conclusion on the solid state reaction between NaNH$_2$ and LiAlH$_4$ in the S-I and S-II samples can be drawn. Scheme 1 summarizes the chemical processes taking place in both systems. In the S-I, the chemical environment of Na changes from NaNH$_2$ to NaAlH$_4$, Li$_3$Na(NH$_2$)$_4$ and finally to NaH; where for Al, it changes from LiAlH$_4$ to NaAlH$_4$, Na$_3$AlH$_6$ and LiAlN$_2$H$_2$. In the S-II, Na changes from NaNH$_2$ to NaAlH$_4$, Li$_3$Na(NH$_2$)$_4$; while Al changes from LiAlH$_4$ to NaAlH$_4$, Li$_3$AlH$_6$ and Li$_2$AlNH$_2$. In the S-II sample a competition between LiAlH$_4$ and NaAlH$_4$ to react with LiNH$_2$ could exist because both complex hydrides present in the system at the earlier stage of dehydrogenation. Because only NaAlH$_4$ was left, the reaction between LiAlH$_4$ and LiNH$_2$ could be more favorable and the dehydrogenation process is thus resulted from the interaction between LiAlH$_4$ and LiNH$_2$. Considering 2 equiv H$_2$ were evolved and assuming NaH and NaAlH$_4$ to be the final Na-containing product in the S-I and S-II samples, the overall reaction occurred in the milling process can be expressed by the reactions (6) and (7).

Scheme 1. Reaction pathways of S-I and S-II samples in the milling process.

$$\text{S-I} \quad \text{LiAlH}_4 + 2\text{NaNH}_2 \rightarrow 2\text{NaH} + [\text{LiAlN}_2\text{H}_2] + 2\text{H}_2 \qquad (6)$$

$$\text{S-II} \quad 2\text{LiAlH}_4 + \text{NaNH}_2 \rightarrow \text{NaAlH}_4 + [\text{Li}_2\text{AlNH}_2] + 2\text{H}_2 \qquad (7)$$
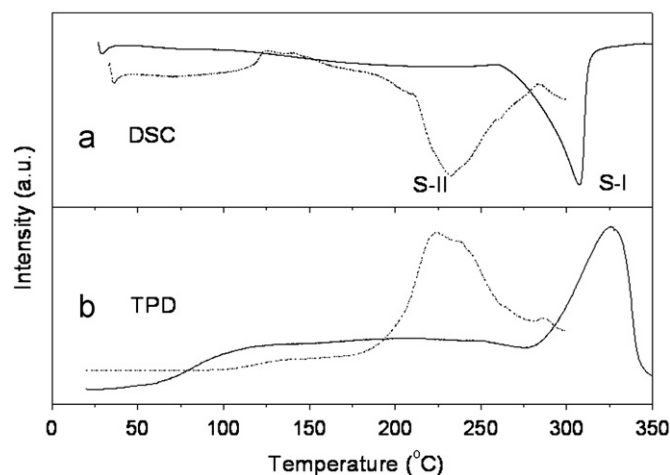
Fig. 6. DSC (a) and TPD (b) measurements on S-I (solid line) and S-II (dash-dot line) samples collected at the end of ball milling.

From the chemical composition point of view, the $LiAlN_2H_2$ formed in the S-I is likely to be a ternary imide of Li and Al, i.e., $LiAl(NH)_2$, which is supported by the observed broadband absorbance centered at $3236 \, cm^{-1}$ in FTIR. In fact, there were reports [25,26] that $LiAl(NH)_2$ could be synthesized through the thermal decomposition of $LiAl(NH_2)_4$. Herein the synthesis process was repeated and the resulting $LiAl(NH)_2$ was found having the same FTIR absorbance with that of $LiAlN_2H_2$. However, the synthesized $LiAl(NH)_2$ is generally amorphous [25] and more experimental evidences are demanded for its presence in the milling residue of S-I. Li_2AlNH_2 complex formed in S-II sample, on the other hand, is likely a mixture of $2LiH+AlN$. Similar results were reported by Dolotko et al. [17] in the investigation of the $LiAlH_4/LiNH_2$ (1/1) system, whereby the dehydrogenation of $[LiAlH_4–LiNH_2]$ during the ball milling was proceeded by two-step reactions:

$$2LiAlH_4+LiNH_2 \rightarrow Li_3AlH_6+AlN+2H_2 \tag{8}$$

$$Li_3AlH_6+LiNH_2 \rightarrow 4LiH+AlN+2H_2 \tag{9}$$
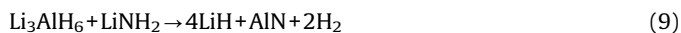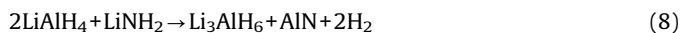
In our study, slight shifts of Li and Al from the LiH (0.54 ppm) and AlN environments (see NMR results in Fig. 5) were observed which could be resulted from the formation of metastable phase between LiH and AlN after undergoing high energetic ball milling.

The thermal decompositions of the solid residues of S-I and S-II were investigated by TPD and DSC. As shown in Fig. 6, the post-milled S-I sample mainly presented two hydrogen signals, the sharp endothermic peak centered at 320 °C characterizes the decomposition of NaH and therefore that broad peak is the result of dehydrogenation of $LiAlN_2H_2$. For the post-milled S-II sample, thermal decomposition of $NaAlH_4$ was observed. The overall observations support the reactions (6) and (7).

4. Conclusion

In this study, $LiAlH_4$–$NaNH_2$ mixtures with $LiAlH_4/NaNH_2$ molar ratio at 1/2 and 2/1 were investigated. It was found that 2 equiv H_2 were desorbed from both mixtures upon ball milling showing the occurrence of interaction between the amide and complex hydride. However, the hydrogen evolutions follow different pathways in above two mixtures. Characterizations on intermediates in the milling revealed that cation exchange takes place at the initial stage of solid state reaction, which leads to the formation of $NaAlH_4$, $Li_3Na(NH_2)_4$ (for S-I and S-II) and $LiNH_2$ (for S-II). The interactions between $NaAlH_4$ with $Li_3Na(NH_2)_4$ and $NaNH_2$ are responsible for hydrogen evolution from S-I sample; while for the S-II sample, the hydrogen mainly comes from the interaction of $LiNH_2$ with $LiAlH_4$. Li–Al–N–H complexes with chemical compositions of $LiAlN_2H_2$ and Li_2AlNH_2 were formed at the end of ball milling in the S-I and S-II, which are ascribed to $LiAl(NH)_2$ imide and a metastable phase formed between LiH and AlN, respectively.

References

[1] B. Bogdanovic, M. Schwickardi, J. Alloys Compd. 253 (1997) 1–9.
[2] G. Sandrock, K. Gross, G. Thomas, J. Alloys Compd. 339 (2002) 299–308.
[3] N.L. Rosi, J. Eckert, M. Eddaoudi, D.T. Vodak, J. Kim, M. O'Keeffe, O.M. Yaghi, Science 300 (2003) 1127–1129.
[4] S.S. Kaye, J.R. Long, J. Am. Chem. Soc. 127 (2005) 6506–6507.
[5] M.E. Bluhm, M.G. Bradley, R. Butterick, U. Kusari, L.G. Sneddon, J. Am. Chem. Soc. 128 (2006) 7748–7749.
[6] A.C. Stowe, W.J. Shaw, J.C. Linehan, B. Schmid, T. Autrey, Phys. Chem. Chem. Phys. 9 (2007) 1831–1836.
[7] P. Chen, Z.T. Xiong, J.Z. Luo, J.Y. Lin, K.L. Tan, Nature 420 (2002) 302–304.
[8] H.Y. Leng, T. Ichikawa, S. Hino, N. Hanada, S. Isobe, H. Fujii, J. Phys. Chem. B 108 (2004) 8763–8765.
[9] Z.T. Xiong, J.J. Hu, G.T. Wu, Y.F. Liu, P. Chen, Catal. Today 120 (2007) 287–291.
[10] T. Ichikawa, N. Hanada, S. Isobe, H.Y. Leng, H. Fujii, J. Phys. Chem. B 108 (2004) 7887–7892.
[11] W.F. Luo, J. Alloys Compd. 381 (2004) 284–287.
[12] P. Chen, Z.T. Xiong, J.Z. Luo, J.Y. Lin, K.L. Tan, J. Phys. Chem. B 107 (2003) 10967–10970.
[13] Z. Xiong, G. Wu, J. Hu, P. Chen, J. Power Sources 159 (2006) 167–170.
[14] Z.T. Xiong, G.T. Wu, J.J. Hu, Y.F. Liu, P. Chen, W.F. Luo, J. Wang, Adv. Funct. Mater. 17 (2007) 1137–1142.
[15] Y. Nakamori, A. Ninomiya, G. Kitahara, M. Aoki, T. Noritake, K. Miwa, Y. Kojima, S. Orimo, J. Power Sources 155 (2006) 447–455.
[16] J. Lu, Z.Z. Fang, J. Phys. Chem. B 109 (2005) 20830–20834.
[17] O. Dolotko, H.Q. Zhang, O. Ugurlu, J.W. Wiench, M. Pruski, L.S. Humbley, V. Pecharsky, Acta Mater. 55 (2007) 3121–3130.
[18] T.N. Dymova, D.P. Aleksandrov, V.N. Konoplev, T.A. Silina, A.S. Sizareva, Koordinatsionnaya Khim. 20 (1994) 279–285.
[19] V.P. Balema, K.W. Dennis, V.K. Pecharsky, Chem. Commun. (2000) 1665–1666.
[20] R.L. Lowton, M.O. Jones, W.I.F. David, S.R. Johnson, M. Sommariva, P.P. Edwards, J. Mater. Chem. 18 (2008) 2355–2360.
[21] Z.T. Xiong, G.T. Wu, J.J. Hu, P. Chen, Adv. Mater. 16 (2004) 1522–1525.
[22] J.W. Wiench, V.P. Balema, V.K. Pecharsky, M. Pruski, J. Solid State Chem. 177 (2004) 648–653.
[23] B. Bogdanovic, M. Felderhoff, M. Germann, M. Hartel, A. Pommerin, F. Schuth, C. Weidenthaler, B. Zibrowius, J. Alloys Compd. 350 (2003) 246–255.
[24] J.J. Fitzgerald, S.D. Kohl, G. Piedra, Chem. Mater. 6 (1994) 1915.
[25] R. Janot, J.B. Eymery, J.M. Tarascon, J. Phys. Chem. C 111 (2007) 2335–2340.
[26] J. Rouxel, R. Brec, C. R. Acad. Sci. Ser. C 262 (1966) 1070.